



# Synthesis, crystal structure, Hirshfeld surface analysis, density function theory calculations and photophysical properties of methyl 4'-[(4-bromobenzoyl)oxy]biphenyl-4-carboxylate: a compound with bromine...oxygen contacts

Hanumaiah Anilkumar,<sup>a</sup> Selvaraj Selvanandan,<sup>b</sup> Metikurke Amruthesh Omkariah,<sup>c</sup> Mahadevaiah Harish Kumar,<sup>d</sup> Hosapalya Thimmaiah Srinivasa<sup>e</sup> and Bandrehalli Siddagangaiah Palakshamurthy<sup>f\*</sup>

Received 13 January 2025

Accepted 21 February 2025

Edited by M. Weil, Vienna University of Technology, Austria

**Keywords:** crystal structure; physical properties; Hirshfeld surface; density function theory; biphenyl-4-carboxylate and solvatochromic.

**CCDC reference:** 2384236

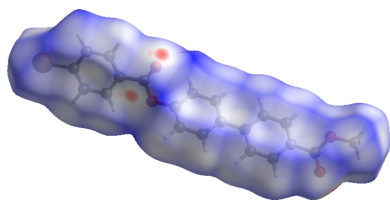
**Supporting information:** this article has supporting information at journals.iucr.org/e

<sup>a</sup>Department of Physics, Government First Grade College, Chikballapur, Karnataka-562101, India, <sup>b</sup>Department of Physics, ACS College of Engineering, Bangalore, Karnataka-560074, India, <sup>c</sup>Department of Physics, Government First Grade College, Kadur, Karnataka-577548, India, <sup>d</sup>Department of Physics, Government Engineering College, Ramanagara, 562159, Karnataka, India, <sup>e</sup>Raman Research Institute, C. V. Raman, Avenue, Sadashivanagar, Bangalore, Karnataka, India, and <sup>f</sup>Department of PG Studies and Research in Physics, Albert Einstein Block, UCS, Tumkur University, Tumkur, Karnataka-572103, India. \*Correspondence e-mail: palaksha.bsmp@gmail.com

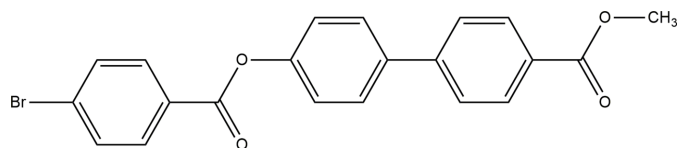
In the molecular title compound, C<sub>21</sub>H<sub>15</sub>BrO<sub>4</sub>, the dihedral angles between the aromatic bromo-benzene ring and the immediate neighbors (first and second aromatic ring of the biphenyl moiety) are 56.57 (2) and 50.91 (4)°. The dihedral angle between the aromatic rings of the biphenyl fragment is 5.78 (4)°. The torsion angles across the ester groups associated with bromo-benzene and methyl moieties are 178.0 (1) and 176.86 (2)°, respectively, revealing an *anti*-periplanar conformation in both cases. In the crystal, the packing of the molecules is stabilized by Br...O contacts running infinitely along [001]. In addition, the crystal packing is consolidated by various C—H... $\pi$  interactions. Hirshfeld surface analysis revealed that the most important contributions to the crystal packing arise from H...H (27.1%), C...H/H...C (39.3%), O...H/H...O (15.4%) and Br...H/H...Br (10.6%) contacts. The net interaction energies for the title compound were computed as  $E_{\text{ele}} = -41.9 \text{ kJ mol}^{-1}$ ,  $E_{\text{pol}} = -11 \text{ kJ mol}^{-1}$ ,  $E_{\text{dis}} = -209.7 \text{ kJ mol}^{-1}$  and  $E_{\text{rep}} = 108.9 \text{ kJ mol}^{-1}$ , with a total interaction energy  $E_{\text{tot}}$  of  $-167.9 \text{ kJ mol}^{-1}$ . The ground-state dipole moment ( $\mu_{\text{g}}$ ) is calculated as 1.2936 debye and the energy gap between HOMO and LUMO orbitals is 4.5203 eV as calculated with density functional theory using the B3LYP/6-31 G level basis set. The electronic absorption and fluorescence spectra of the compound were recorded and studied in different solvents by varying polarity. These results were used to elucidate the solvatochromic properties, and spectral deviations were studied by the linear solvation energy relationship. Lippert, Bakshiev, and Bilot-Kawski-Chamma-Viallet equations were used to estimate the ground and excited-state dipole moments ( $\mu_{\text{e}}$ ). The excited dipole moment is found to be higher than the ground state dipole moment, which indicates that  $\pi$ -electrons are more distributed in polar excited molecules.

## 1. Chemical context

Molecules derived from biphenyl are found to exhibit liquid-crystal properties because of their linearity, high symmetry and thermal stability (Ranganathan & Ramesh, 2006; Imai *et al.*, 2001). The thermotropic liquid crystalline phases containing biphenyl moieties have an ability to form ordered structures so that they have been widely studied in recent decades (Bagheri *et al.*, 2004). The methylene entity that is directly attached to biphenyl mesogens undergoes self-poly-



condensation, revealing smectic (Sm) A and B phases (Nakata & Watanabe, 1994). The absence of alkyl chains/highly polar groups at the ends in the molecular structures of liquid crystals induces non-liquid crystal properties (Harish Kumar *et al.*, 2024b). Rigid cores such as cyclic  $\pi$ - or heterocyclic  $\pi$ -systems are responsible for electro-optical phenomena. For example, biphenyl-4-carboxylate derivatives are found to exhibit liquid-crystal properties, which play an important role in electro-optical phenomena caused by weak electric fields (Mikulko *et al.*, 2006). It is well known that molecules derived from conjugated biphenyl-4-carboxylate exhibit optical non-linearity, especially when they have donor and acceptor substituents at each end of the molecular systems. This originates from an efficient intramolecular charge transfer through a highly polarizable  $\pi$ -electron system. The electro-optical response depends on the structure, sample thickness, birefringence, light absorption, scattering and other factors. Therefore, the results of electro-optical measurements are in most cases arbitrary and, consequently, the absolute values of neither linear nor higher order electro-optical coefficients can be determined (Dardas *et al.*, 2009). However, the knowledge of linear and non-linear electro-optical coefficients are required to study the material response to an applied electric field. In this scenario it is necessary to look at the dipole moment, which has an influence on the refractive index or polarization changes at high electric field. Keeping this in mind, we made an attempt to synthesize corresponding phases and report here on the crystal structure analysis, solvatochromism response and dipole moment of the title compound,  $C_{21}H_{15}BrO_4$ , (I).



## 2. Structural commentary

The molecular structure of (I) is shown in Fig. 1. The dihedral angles between the bromobenzene and the aromatic rings (C8–C13) and (C14–C19) of the biphenyl moiety are 56.57 (2) and 50.91 (4)°, respectively, whereas the dihedral angle between the two aromatic rings of the biphenyl moiety is

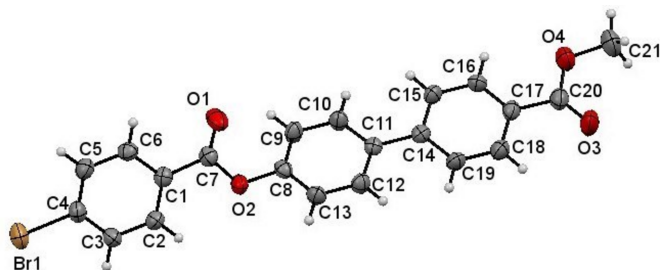


**Figure 1**

The molecular structure of (I), showing displacement ellipsoids at the 50% probability level.

**Table 1**

Hydrogen-bond geometry (Å, °).

$Cg1$ ,  $Cg2$  and  $Cg3$  are the centroids of the aromatic rings C1–C6, C8–C13 and C14–C19, respectively

$D-H\cdots A$	$D-H$	$H\cdots A$	$D\cdots A$	$D-H\cdots A$
C3–H3 $\cdots$ Cg1 <sup>i</sup>	0.93	2.82	3.526 (4)	133
C6–H6 $\cdots$ Cg1 <sup>ii</sup>	0.93	2.83	3.523 (4)	133
C10–H10 $\cdots$ Cg2 <sup>iii</sup>	0.93	2.83	3.523 (4)	132
C13–H13 $\cdots$ Cg2 <sup>iv</sup>	0.93	2.87	3.552 (4)	131
C16–H16 $\cdots$ Cg3 <sup>iii</sup>	0.93	2.92	3.566 (4)	128
C19–H19 $\cdots$ Cg3 <sup>iv</sup>	0.93	2.99	3.623 (4)	127

Symmetry codes: (i)  $x - \frac{1}{2}, -y - \frac{1}{2}, z$ ; (ii)  $x + \frac{1}{2}, -y + \frac{3}{2}, z$ ; (iii)  $x + \frac{1}{2}, -y + \frac{1}{2}, z$ ; (iv)  $x - \frac{1}{2}, -y + \frac{3}{2}, z$ .

5.78 (4)°. The torsion angles involving the biphenyl moiety and the attached ester groups are 178.0 (3)° (C1–C7–O2–C8) and 176.9 (4)° (C17–C20–O4–C21), respectively, making the conformation *anti*-periplanar in both cases.

## 3. Supramolecular features

The crystal packing is stabilized by a halogen–oxygen (Br $\cdots$ O) interaction C–Br1 $\cdots$ O3–C with a Br $\cdots$ O distance of 3.105 (2) Å, forming infinite chains running parallel to [001] (Fig. 2). The packing is further consolidated by six C–H $\cdots$  $\pi$  interactions between aromatic CH groups and the centroids (Cg) of adjacent aromatic rings (Table 1), as illustrated in Fig. 3.

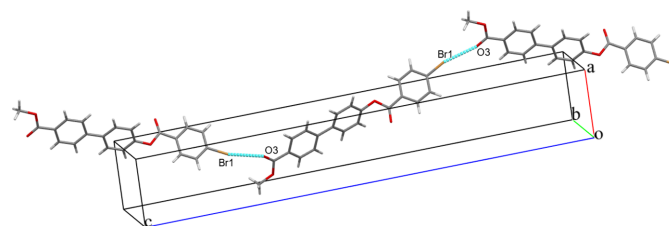


**Figure 2**

The molecular packing of (I). Dashed lines indicate Br $\cdots$ O interactions.

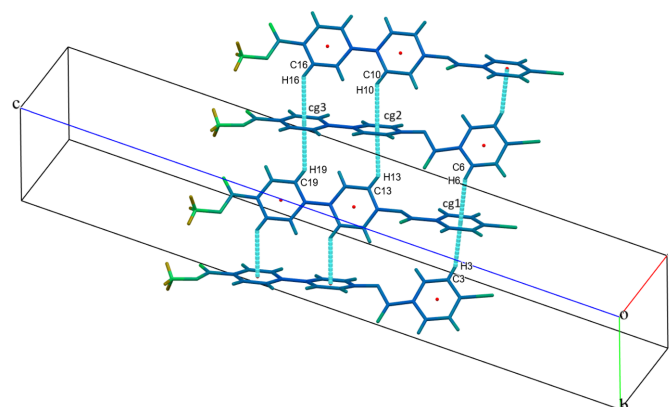


**Figure 3**

The molecular packing of (I). Dashed lines indicate C–H $\cdots$ Cg interactions.

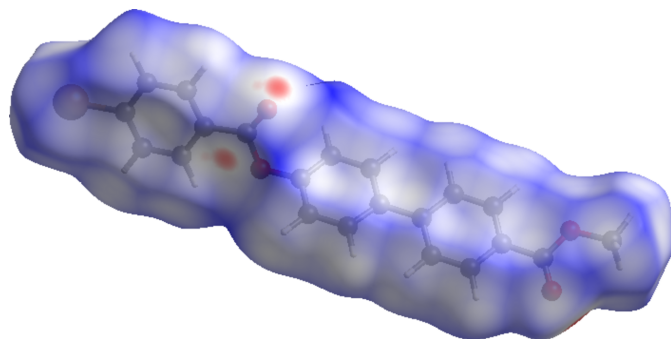


**Figure 4**  
Hirshfeld surface of (I) mapped with  $d_{\text{norm}}$ .

#### 4. Database survey

A search of the Cambridge Structural Database (CSD, version 5.42, update of November 2020; Groom *et al.*, 2016) for molecules containing the biphenyl carboxylate fragment resulted in more than thirty matches, with molecular features similar to (I) for compounds with refcodes DEZYUF (Ardeleanu *et al.*, 2018), DOJLIB (Lin *et al.*, 2024), FIRYEN (Royal & Baudoin, 2019) and VUCFEI (Harish Kumar *et al.*, 2024a). In these compounds, the dihedral angle between the aromatic rings of the biphenyl moieties are in the range of 33.07 (3) to 38.14 (5)°. They have simple substituent groups at one end of the biphenyl moiety. Compounds with refcodes COFMET (Cai *et al.*, 2024), ASUJAB (Lustig *et al.*, 2016), CUXCAC (Das *et al.*, 2021) all have substituents in the biphenyl fragments, with dihedral angles between the aromatic rings of the biphenyl moiety in the range 44.04 (3) to 51.06 (2)°. It is quite characteristic that the dihedral angle between unsubstituted biphenyl rings are around 30 to 45° due to steric hindrance between *ortho*-hydrogen atoms of each ring. The small value of 5.78 (4)° for the dihedral angle found in the title compound is due to the presence of bulky groups at each end of the molecule and the interactions resulting from halogen...oxygen contacts at one end of the biphenyl moiety.

#### 5. Hirshfeld surface analysis

Hirshfeld surface analysis was carried out using *Crystal-Explorer* (Spackman *et al.*, 2021) to quantify the various

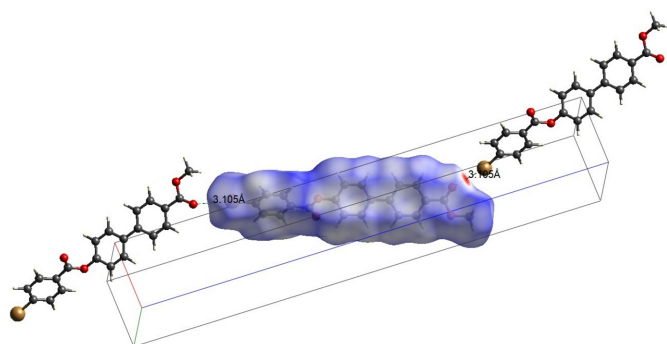


**Figure 5**  
Hirshfeld surface of (I) mapped with  $d_{\text{norm}}$ . The dashed lines indicate Br...O interactions running parallel [001].

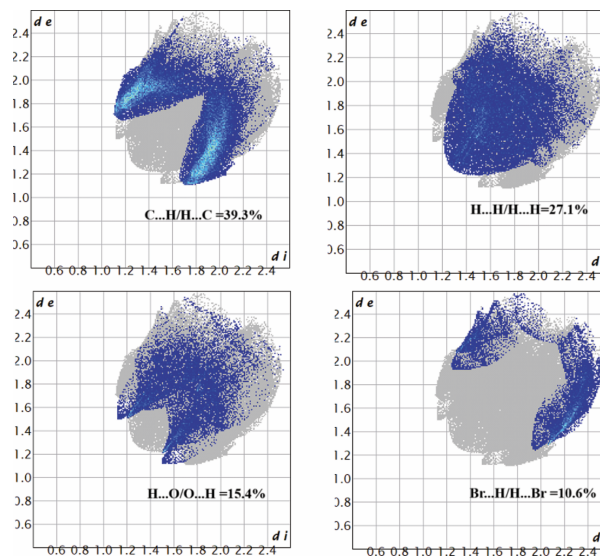


**Figure 6**  
Two-dimensional fingerprint plots for (I).

intermolecular interaction present in (I). Fig. 4 illustrates the Hirshfeld surface mapped with  $d_{\text{norm}}$  where red spots near the oxygen atom of the surface correspond to the short contacts in the molecule. The Br...O contact associated with electrophilic region of the Hirshfeld surface is shown in Fig. 5. The two-dimensional fingerprint plots (Fig. 6) reveal that the major contributions to the crystal packing are from H...H/H...H (27.1%), C...H/H...C (39.3%), O...H/H...O (15.4%) and Br...H/H...Br (10.6%) contacts.

Energy framework calculations were performed using the basis set B3LYP/6-31G(d,p). The net interaction energies for the title compound are  $E_{\text{ele}} = -41.9 \text{ kJ mol}^{-1}$ ,  $E_{\text{pol}} = -11 \text{ kJ mol}^{-1}$ ,  $E_{\text{dis}} = -209.7 \text{ kJ mol}^{-1}$  and  $E_{\text{rep}} = 108.9 \text{ kJ mol}^{-1}$ , with a total interaction energy  $E_{\text{tot}}$  of  $-167.9 \text{ kJ mol}^{-1}$ , which shows that  $E_{\text{dis}}$  is the major interaction. The energy framework showing the electrostatic (coulomb) potential force, the dispersion force and the total energy diagram are shown in Fig. 7.

#### 6. Density functional theory (DFT) calculations

DFT calculations were carried out using *Gaussian-09W* (Frisch *et al.*, 2009), with *Gaussian View 5.0* used to generate the optimized structure of (I). The optimized parameters of the title compound were obtained using the B3LYP/6-311G (d, p) basis set. The dipole moment of the molecule in the gaseous phase was computed to be 1.2936 debye, and is illustrated in Fig. 8. Furthermore, the frontier molecular orbitals HOMO and LUMO of (I) were computed, with energies of HOMO and LUMO of  $-6.2450$  and  $-1.7246 \text{ eV}$ , respectively (the energy gap  $\Delta E$  is 4.5203 eV; Fig. 9). The molecular electrostatic potential (MEP) surface of the optimized structure is shown in Fig. 10. The nucleophilic and electrophilic reactive sites of (I) are represented by red and blue regions on the MEP surface. For (I), the red area covers the oxygen atoms of

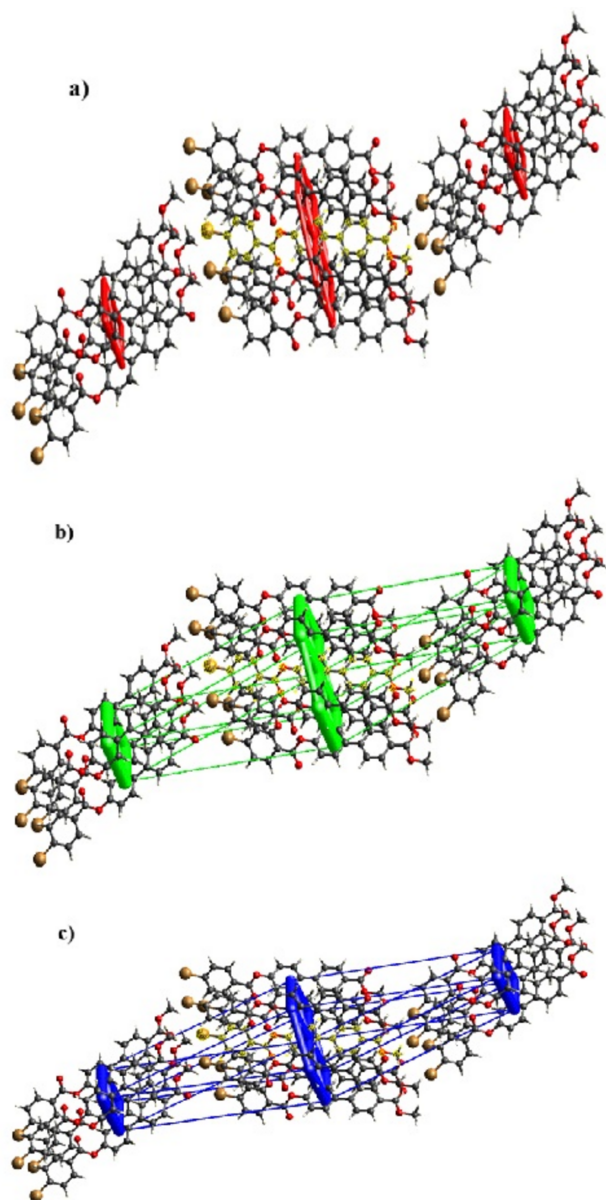


**Figure 7**  
Energy frameworks calculated for (I), viewed along [100], showing (a) Coulomb potential force, (b) dispersion force and (c) total energy diagrams. The cylindrical radii are proportional to the relative strength of the corresponding energies (adjusted to a cutoff value of  $5 \text{ kJ mol}^{-1}$ ).

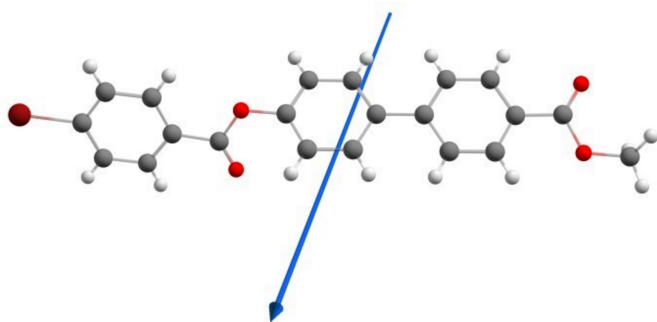


**Figure 8**  
The direction of the dipole moment of (I) in the gaseous phase indicated by the arrow.

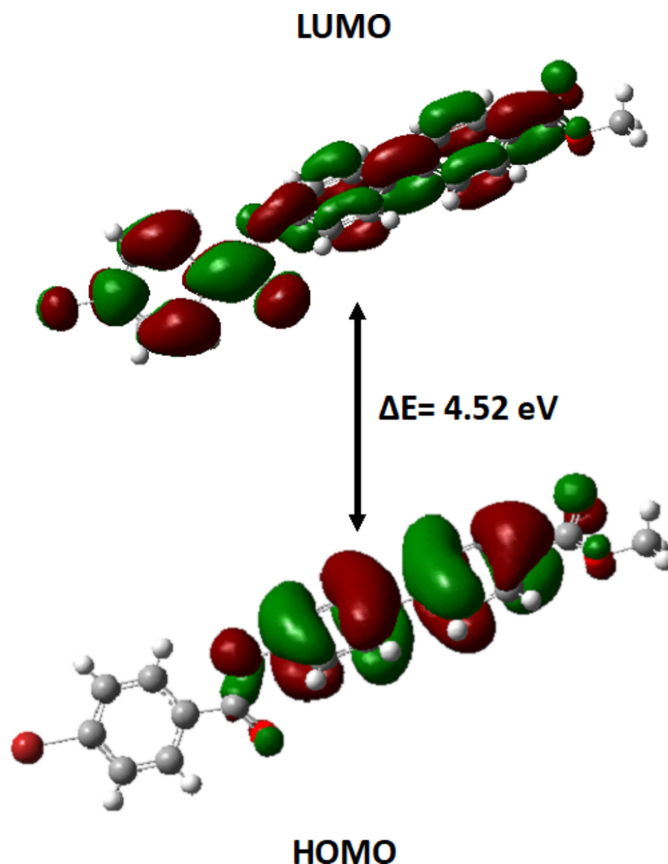


**Figure 9**  
HOMO and LUMO of (I) with the energy band gap  $E_g$ .

the ester functionality, revealing the sensitivity towards nucleophilic attack. The pale blue area around the aromatic rings indicates weak electrophilic sites.

## 7. Photophysical properties

The photophysical properties of (I) were estimated by the solvatochromism method (Reichardt & Welton, 2011). The absorption spectra in different polar liquids were recorded, and intensity maxima observed between 285 and 288 nm (Fig. 11). Since the solvent polarity is susceptible to longer wavelength absorption, the samples were excited at longer wavelength to get emission spectra for calculation of the photophysical parameters. The ground state and experimental excited dipole moments were derived according to Lippert

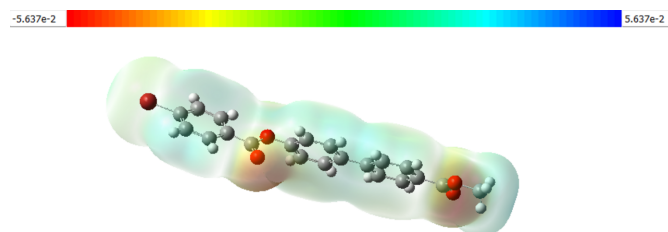


**Figure 10**  
MEP surface plots of (I); regions of attractive potential appear in red and those of repulsive potential appear in blue.

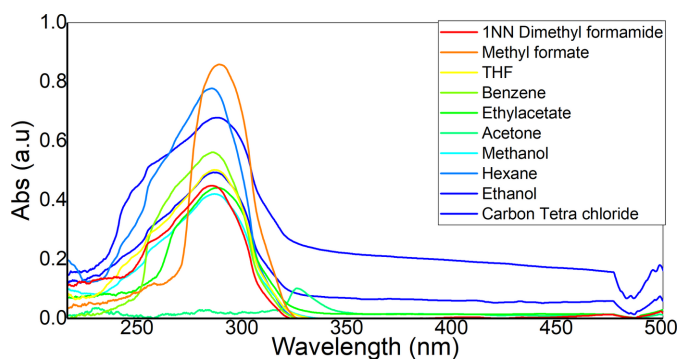


**Figure 11**  
The absorption spectra of (I) recorded in different solvents.

(1957), Bakhshiev (1964) and Bilot–Kawski–Chamma–Viallet (Bilot & Kawski, 1963; Chamma & Viallet, 1970) polarity functions, as detailed in equations (1)–(3). Among these, Bakhshiev and Bilot–Kawski–Chamma–Viallet equations give good results with reduced errors in the calculation. Fig. 12

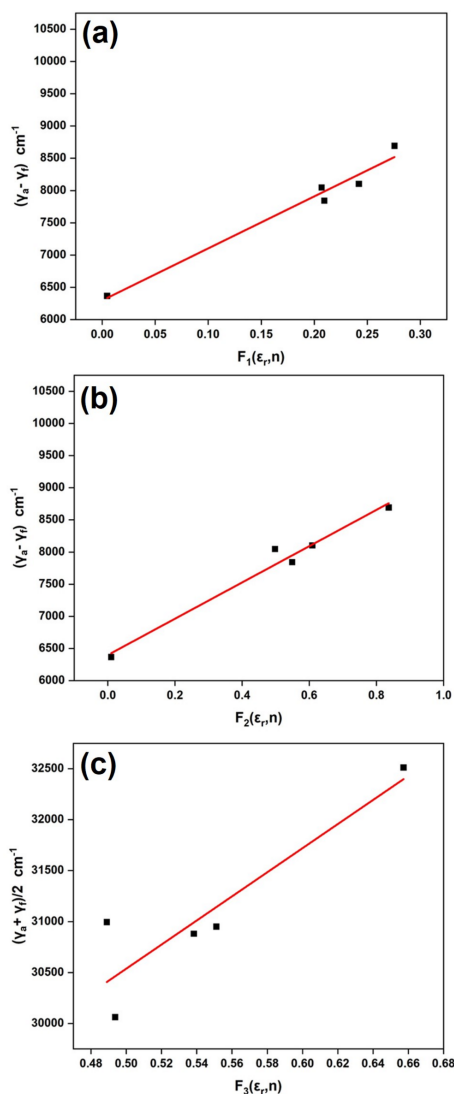


**Figure 12**  
The variation of Stokes shift according to the (a) Lippert, (b) Bakshiev and (c) Bilot–Kawski–Chamma–Viallet functions in different solvents.

shows  $\bar{\nu}_a \bar{\nu} - \bar{\nu}_f$  versus  $F_1(\epsilon, n)$ ,  $\bar{\nu}_a - \bar{\nu}_f$  versus  $F_2(\epsilon, n)$  and  $(\bar{\nu}_a + \bar{\nu}_f)/2$  versus  $F_3(\epsilon, n)$ , resulting in linear graphs with slopes  $m_1$ ,  $m_2$  and  $m_3$ , respectively.

$$\bar{\nu}_a - \bar{\nu}_f = m_1 F_1 + \text{constant}, \quad (1)$$

$$\bar{\nu}_a - \bar{\nu}_f = m_2 F_2 + \text{constant}, \quad (2)$$

$$\frac{\bar{\nu}_a + \bar{\nu}_f}{2} = m_3 F_3 + \text{constant}. \quad (3)$$

The expressions for the Lippert polarity [ $F_1(\epsilon, n)$ ], Bakhshiev polarity [ $F_2(\epsilon, n)$ ] and Bilot–Kawski–Chamma–Viallet [ $F_3(\epsilon, n)$ ] polarity functions are given by equations (4)–(6):

$$F_1(\epsilon, n) = \left[ \frac{\epsilon - 1}{2\epsilon + 1} - \frac{n^2 - 1}{2n^2 + 1} \right], \quad (4)$$

$$F_2(\epsilon, n) = \frac{2n^2 + 1}{n^2 + 2} \left[ \frac{\epsilon - 1}{\epsilon + 2} - \frac{n^2 - 1}{n^2 + 2} \right], \quad (5)$$

$$F_3(\epsilon, n) = \left[ \frac{2n^2 + 1}{2(n^2 + 2)} \left( \frac{\epsilon - 1}{\epsilon + 2} - \frac{n^2 - 1}{n^2 + 2} \right) + \frac{3(n^4 - 1)}{2(n^2 + 2)^2} \right], \quad (6)$$

where  $\bar{\nu}_a$  and  $\bar{\nu}_f$  are the absorption and fluorescence maxima wavenumbers in  $\text{cm}^{-1}$ , respectively;  $n$  is the refractive index and  $\epsilon$  is the permittivity. The slopes  $m_1$ ,  $m_2$ ,  $m_3$  are connected with ground and excited state dipole moments through equations (7)–(9):

$$m_1 = \frac{2(\mu_e - \mu_g)^2}{hca_0^3}, \quad (7)$$

$$m_2 = \frac{2(\mu_e - \mu_g)^2}{hca_0^3}, \quad (8)$$

$$m_3 = \frac{2(\mu_e^2 - \mu_g^2)}{hca_0^3}, \quad (9)$$

where  $\mu_e$  and  $\mu_g$  are the excited and ground state dipole moments of the solute molecule ( $h$  and  $c$  are Planck's constant and velocity of light in a vacuum, respectively);  $a_0$  is the Onsager cavity radius of the title compound as determined by Suppan's equation  $a_0 = (3M/4\pi\delta N)^{1/3}$  where  $\delta$  is the density of the solute molecule,  $M$  is molecular weight and  $N$  is Avogadro's number.

$$\mu_g = \frac{|m_3 - m_2|}{2} \left( \frac{hca_0^3}{2m_2} \right)^{1/2}, \quad (10)$$

$$\mu_e = \frac{|m_3 + m_2|}{2} \left( \frac{hca_0^3}{2m_2} \right)^{1/2}, \quad (11)$$

$$\frac{\mu_e}{\mu_g} = \frac{|m_3 + m_2|}{|m_3 - m_2|}. \quad (12)$$

The solvent polarity function values  $F_1(\epsilon, n)$ ,  $F_2(\epsilon, n)$ , and  $F_3(\epsilon, n)$  of various solvents on the band shift data of the title compound is summarized in Table 2. The slopes and intercepts

**Table 2**  
Solvatochromic data for (I) ( $\text{cm}^{-1}$ ) with calculated values of  $F_1$ ,  $F_2$  and  $F_3$ .

Solvent	$\bar{\nu}_a$	$\bar{\nu}_f$	$\bar{\nu}_a - \bar{\nu}_f$	$(\bar{\nu}_a + \bar{\nu}_f)/2$	$F_1(\epsilon, n)$	$F_2(\epsilon, n)$	$F_3(\epsilon, n)$
Hexane	35018.66	25278.69	9739.96	30148.68	0.0010	0.0018	0.2540
Methyl formate	34931.50	26829.07	8102.43	30880.29	0.2421	0.6091	0.5383
Benzene	34580.37	28213.51	6366.85	31396.94	0.0045	0.0099	0.3430
THF	34872.48	27029.94	7842.53	30951.21	0.2095	0.5490	0.5511
$\text{CCl}_4$	34665.78	25457.60	9208.18	30061.69	0.1434	0.3632	0.4936
Ethyl acetate	35018.66	26970.89	8047.76	30994.78	0.1996	0.4890	0.4979
Acetone	30659.54	28696.87	1962.67	29678.21	0.2841	0.7902	0.6395
Methanol	34872.48	30151.35	4721.12	32511.92	0.3083	0.8545	0.6514
Ethanol	34872.48	24628.11	10244.37	29750.30	0.2888	0.8129	0.6523
Dimethyl formamide	34665.782	25972.67	8693.10	30319.229	0.2757	0.8368	0.7077

**Table 3**  
Statistical treatment of the correlations of solvent spectroscopic shifts of the title compound.

Method	Slope	Intercept	Correlation coefficient	Number of data
Lippert correlation	8054	6928	0.97	5
Bakhshiev correlation	2820	6398	0.97	5
Bilot–Kawaski–Chamma–Viallet correlation	8626	24622	0.82	5

**Table 4**  
Ground and excited states dipole moments of (I) (in debye<sup>a</sup>).

Molecule	Radius $a$ (Å)	$\mu_g^b$ (D)	$\mu_e^c$ (D)	$\mu_e^d$ (D)	$(\mu_e/\mu_g)^e$ (D)
(I)	4.6	1.2936	5.37	10.59	1.97

of the fitted lines are given in Table 3 with good correlation coefficients obtained in all cases. The ground state and excited state dipole moments were estimated by the above equations under assumption that the symmetry of (I) remains unchanged upon electronic transition. The ground and excited dipole moments are found to be parallel according to equations (8) and (9). This part of the study demonstrates that the title compound is more polar in the excited state than in the ground state for all the solvents. The ratio of the dipole moments can be determined by Stokes shifts in different solvents as functions of  $\epsilon$  and  $n$ . The calculated values for (I) are collated in Table 4.

## 8. Synthesis and crystallization

4-Bromobenzoic acid (1 equiv.) was reacted with methyl 4'-hydroxy-[1,1'-biphenyl]-4-carboxylate (1 equiv.) in dry chloroform in the presence of dicyclohexylcarbodiimide (1.2 equiv.) and a catalytic quantity of dimethyl aminopyrimidine at room temperature for about 12 h. After completion of the reaction, the mixture was poured into water and extracted into chloroform. The organic solvent was washed with water (10 ml), dilute acetic acid (10 ml) and dried over sodium sulfate. The crude final product was recrystallized from chloroform at room temperature.

## 9. Refinement details

Crystal data, data collection and structure refinement details are summarized in Table 5. The structure was refined as a two-component inversion twin. All H atoms were positioned with

idealized geometry and refined using a riding model with  $\text{C}—\text{H} = 0.93–0.96$  Å and  $U_{\text{iso}}(\text{H}) = 1.2–1.5U_{\text{eq}}(\text{C})$ .

**Table 5**  
Experimental details.

Crystal data	
Chemical formula	$\text{C}_{21}\text{H}_{15}\text{BrO}_4$
$M_r$	411.24
Crystal system, space group	Orthorhombic, $Pna2_1$
Temperature (K)	300
$a, b, c$ (Å)	5.9754 (8), 7.2962 (9), 39.537 (5)
$V$ (Å <sup>3</sup> )	1723.7 (4)
$Z$	4
Radiation type	Mo $K\alpha$
$\mu$ (mm <sup>-1</sup> )	2.41
Crystal size (mm)	0.28 × 0.24 × 0.21
Data collection	
Diffractometer	Bruker SMART APEXII CCD
Absorption correction	Multi-scan (SADABS; Krause <i>et al.</i> , 2015)
$T_{\text{min}}, T_{\text{max}}$	0.152, 0.601
No. of measured, independent and observed [ $I > 2\sigma(I)$ ] reflections	41401, 5204, 4189
$R_{\text{int}}$	0.039
$(\sin \theta/\lambda)_{\text{max}}$ (Å <sup>-1</sup> )	0.715
Refinement	
$R[F^2 > 2\sigma(F^2)], wR(F^2), S$	0.035, 0.072, 1.05
No. of reflections	5204
No. of parameters	236
No. of restraints	1
H-atom treatment	H-atom parameters constrained
$\Delta\rho_{\text{max}}, \Delta\rho_{\text{min}}$ (e Å <sup>-3</sup> )	0.27, -0.46
Absolute structure	Refined as an inversion twin
Absolute structure parameter	0.060 (11)

Computer programs: APEX2 and SAINT (Bruker, 2017), SHELXT (Sheldrick, 2015a), SHELXL (Sheldrick, 2015b), Mercury (Macrae *et al.*, 2020) and publCIF (Westrip, 2010).

### Acknowledgements

The authors thank the Vision Group on Science and Technology, Government of Karnataka, for the award of a major project under the CISEE scheme (reference No. VGST/CISEE/GRD-319/2014–15) to carry out this work at the Department of PG Studies and Research in Physics, UCS, Tumkur University.

### Funding information

Funding for this research was provided by: Vision Group on Science and Technology, Government of Karnataka (grant No. VGST/CISEE/GRD-319/2014–15 to Palakshamurthy B. S).

### References

- Ardeleanu, R., Dascălu, A., Shova, S., Nicolescu, A., Roşca, I., Bratanovici, B. I., Lozan, V. & Roman, G. (2018). *J. Mol. Struct.* **1173**, 63–71.
- Bagheri, M., Didehban, K., Rezvani, Z. & Akbar Entezami, A. (2004). *Eur. Polym. J.* **40**, 865–871.
- Bakhshiev, N. G. (1964). *Opt. Spektrosc.* **16**, 821–832.
- Bilot, L. & Kawski, A. (1963). *Z. Naturforsch. Teil A*, **17**, 621–627.
- Bruker (2017). *APEX2* and *SAINT*. Bruker AXS Inc., Madison, Wisconsin, USA.
- Cai, X., Ding, D., Zhao, S., Wen, S., Zhang, G., Bai, P. & Xu, C. (2024). *Inorg. Chem.* **63**, 2313–2321.
- Chamma, A. & Viallet, P. (1970). *Acad. C. R. Sci. Paris, Ser. C*, **270**, 1901–1904.
- Dardas, D., Kuczyński, W., Hoffmann, J., Jeżewski, W., Nowicka, K. & Malecki, J. (2009). *Opto-Electron. Rev.* **17**, 25–29.
- Das, T., Mohar, M. & Bag, A. (2021). *Tetrahedron Lett.* **65**, 152750.
- Frisch, M. J., Trucks, G. W., Schlegel, H. B., Scuseria, G. E., Robb, M. A., Cheeseman, J. R., Scalmani, G., Barone, V., Mennucci, B., Petersson, G. A., Nakatsuji, H., Caricato, M., Li, X., Hratchian, H. P., Izmaylov, A. F., Bloino, J., Zheng, G., Sonnenberg, J. L., Hada, M., Ehara, M., Toyota, K., Fukuda, R., Hasegawa, J., Ishida, M., Nakajima, T., Honda, Y., Kitao, O., Nakai, H., Vreven, T., Montgomery, J. A. Jr, Peralta, J. E., Ogliaro, F., Bearpark, M., Heyd, J. J., Brothers, E., Kudin, K. N., Staroverov, V. N., Kobayashi, R., Normand, J., Raghavachari, K., Rendell, A., Burant, J. C., Iyengar, S. S., Tomasi, J., Cossi, M., Rega, N., Millam, J. M., Klene, M., Knox, J. E., Cross, J. B., Bakken, V., Adamo, C., Jaramillo, J., Gomperts, R., Stratmann, R. E., Yazyev, O., Austin, A. J., Cammi, R., Pomelli, C., Ochterski, J. W., Martin, R. L., Morokuma, K., Zakrzewski, V. G., Voth, G. A., Salvador, P., Dannenberg, J. J., Dapprich, S., Daniels, A. D., Farkas, O., Foresman, J. B., Ortiz, J. V., Cioslowski, J. & Fox, D. J. (2009). *Gaussian 09W*, Revision A. 02. Gaussian, Inc., Wallingford CT, USA.
- Groom, C. R., Bruno, I. J., Lightfoot, M. P. & Ward, S. C. (2016). *Acta Cryst.* **B72**, 171–179.
- Harish Kumar, M., Santhosh Kumar, S., Devarajegowda, H. C., Srinivasa, H. T. & Palakshamurthy, B. S. (2024b). *Acta Cryst.* **E80**, 1180–1185.
- Harish Kumar, M., Vinduvahini, M., Devarajegowda, H. C., Srinivasa, H. T. & Palakshamurthy, B. S. (2024a). *Acta Cryst.* **E80**, 1010–1013.
- Imai, Y., Takeuchi, A., Watanabe, S., Kakimoto, M. A. & Kurosaki, T. (2001). *Macromol. Chem. Phys.* **202**, 26–30.
- Krause, L., Herbst-Irmer, R., Sheldrick, G. M. & Stalke, D. (2015). *J. Appl. Cryst.* **48**, 3–10.
- Lin, H., Yang, Y., Diamond, B. G., Yan, T. H., Bakhmutov, V. I., Festus, K. W., Cai, P., Xiao, Z., Leng, M., Afolabi, I., Day, G. S., Fang, L., Hendon, C. H. & Zhou, H. C. (2024). *J. Am. Chem. Soc.* **146**, 1491–1500.
- Lippert, E. (1957). *Z. Elektrochem.* **61**, 962–975.
- Lustig, W. P., Wang, F., Teat, S. J., Hu, Z., Gong, Q. & Li, J. (2016). *Inorg. Chem.* **55**, 7250–7256.
- Macrae, C. F., Sovago, I., Cottrell, S. J., Galek, P. T. A., McCabe, P., Pidcock, E., Platings, M., Shields, G. P., Stevens, J. S., Towler, M. & Wood, P. A. (2020). *J. Appl. Cryst.* **53**, 226–235.
- Mikulko, A., Marzec, M., Wróbel, S. & Dąbrowski, R. (2006). *Opto-Electron. Rev.* **14**, 319–322.
- Nakata, Y. & Watanabe, J. (1994). *J. Mater. Chem.* **4**, 1699–1703.
- Ranganathan, T. & Ramesh, C. (2006). *React. Funct. Polym.* **66**, 1003–1013.
- Reichardt, C. & Welton, T. (2011). *Solvents and solvent effects in organic chemistry*. John Wiley & Sons.
- Royal, T. & Baudoin, O. (2019). *Chem. Sci.* **10**, 2331–2335.
- Sheldrick, G. M. (2015a). *Acta Cryst.* **A71**, 3–8.
- Sheldrick, G. M. (2015b). *Acta Cryst.* **C71**, 3–8.
- Spackman, P. R., Turner, M. J., McKinnon, J. J., Wolff, S. K., Grimwood, D. J., Jayatilaka, D. & Spackman, M. A. (2021). *J. Appl. Cryst.* **54**, 1006–1011.
- Westrip, S. P. (2010). *J. Appl. Cryst.* **43**, 920–925.

## supporting information

*Acta Cryst.* (2025). E81, 264-270 [https://doi.org/10.1107/S2056989025001604]

## Synthesis, crystal structure, Hirshfeld surface analysis, density function theory calculations and photophysical properties of methyl 4'-[(4-bromobenzoyl)-oxy]biphenyl-4-carboxylate: a compound with bromine...oxygen contacts

Hanumaiah Anilkumar, Selvaraj Selvanandan, Metikurke Amruthesh Omkariah, Mahadevaiah Harish Kumar, Hosapalya Thimmaiah Srinivasa and Bandrehalli Siddagangaiah Palakshamurthy

### Computing details

#### Methyl 4'-[(4-bromobenzoyl)oxy]biphenyl-4-carboxylate

##### Crystal data

C<sub>21</sub>H<sub>15</sub>BrO<sub>4</sub>

*M<sub>r</sub>* = 411.24

Orthorhombic, *Pna*2<sub>1</sub>

Hall symbol: P 2c -2n

*a* = 5.9754 (8) Å

*b* = 7.2962 (9) Å

*c* = 39.537 (5) Å

*V* = 1723.7 (4) Å<sup>3</sup>

*Z* = 4

*F*(000) = 832

*D<sub>x</sub>* = 1.585 Mg m<sup>-3</sup>

Melting point: 460 K

Mo *Kα* radiation, λ = 0.71073 Å

Cell parameters from 4189 reflections

θ = 2.8–30.0°

μ = 2.41 mm<sup>-1</sup>

*T* = 300 K

Prism, colourless

0.28 × 0.24 × 0.21 mm

##### Data collection

Bruker SMART APEXII CCD  
diffractometer

Radiation source: fine-focus sealed tube

Graphite monochromator

Detector resolution: 1.02 pixels mm<sup>-1</sup>

φ and Ω scans

Absorption correction: multi-scan  
(SADABS; Krause *et al.*, 2015)

*T<sub>min</sub>* = 0.152, *T<sub>max</sub>* = 0.601

41401 measured reflections

5204 independent reflections

4189 reflections with *I* > 2σ(*I*)

*R<sub>int</sub>* = 0.039

θ<sub>max</sub> = 30.6°, θ<sub>min</sub> = 2.8°

*h* = -8→8

*k* = -10→10

*l* = -55→56

##### Refinement

Refinement on *F*<sup>2</sup>

Least-squares matrix: full

*R*[*F*<sup>2</sup> > 2σ(*F*<sup>2</sup>)] = 0.035

*wR*(*F*<sup>2</sup>) = 0.072

*S* = 1.05

5204 reflections

236 parameters

1 restraint

0.12 constraints

Primary atom site location: structure-invariant  
direct methods

Secondary atom site location: difference Fourier  
map

Hydrogen site location: inferred from  
neighbouring sites

H-atom parameters constrained

*w* = 1/[σ<sup>2</sup>(*F<sub>o</sub>*<sup>2</sup>) + (0.0182*P*)<sup>2</sup> + 0.6795*P*]

where *P* = (*F<sub>o</sub>*<sup>2</sup> + 2*F<sub>c</sub>*<sup>2</sup>)/3

$$(\Delta/\sigma)_{\max} < 0.001$$

$$\Delta\rho_{\max} = 0.27 \text{ e } \text{\AA}^{-3}$$

$$\Delta\rho_{\min} = -0.46 \text{ e } \text{\AA}^{-3}$$

Absolute structure: Refined as an inversion twin  
 Absolute structure parameter: 0.060 (11)

#### Special details

**Geometry.** All esds (except the esd in the dihedral angle between two l.s. planes) are estimated using the full covariance matrix. The cell esds are taken into account individually in the estimation of esds in distances, angles and torsion angles; correlations between esds in cell parameters are only used when they are defined by crystal symmetry. An approximate (isotropic) treatment of cell esds is used for estimating esds involving l.s. planes.

**Refinement.** Refined as a 2-component inversion twin.

#### Fractional atomic coordinates and isotropic or equivalent isotropic displacement parameters ( $\text{\AA}^2$ )

	x	y	z	$U_{\text{iso}}^*/U_{\text{eq}}$
Br1	1.33516 (7)	0.54905 (5)	0.28015 (2)	0.05786 (12)
O2	0.9870 (4)	0.5141 (3)	0.44334 (6)	0.0385 (5)
O1	0.6870 (4)	0.3799 (4)	0.41979 (7)	0.0572 (7)
C21	0.1186 (9)	0.5432 (8)	0.71793 (12)	0.0705 (15)
H21A	-0.031918	0.589171	0.717313	0.106*
H21B	0.117386	0.417942	0.725346	0.106*
H21C	0.205866	0.615516	0.733346	0.106*
O4	0.2160 (5)	0.5539 (4)	0.68434 (7)	0.0606 (8)
C20	0.4255 (7)	0.4952 (5)	0.68076 (10)	0.0447 (8)
C17	0.5027 (6)	0.5032 (5)	0.64515 (8)	0.0364 (7)
C18	0.7117 (6)	0.4322 (5)	0.63731 (9)	0.0414 (8)
H18	0.801659	0.385070	0.654425	0.050*
C19	0.7869 (5)	0.4308 (5)	0.60442 (9)	0.0390 (7)
H19	0.927359	0.382180	0.599737	0.047*
C14	0.6585 (5)	0.5002 (4)	0.57790 (8)	0.0304 (6)
C11	0.7408 (5)	0.5000 (4)	0.54250 (8)	0.0296 (6)
C12	0.9405 (6)	0.4156 (5)	0.53322 (8)	0.0375 (7)
H12	1.024510	0.356560	0.549743	0.045*
C13	1.0183 (6)	0.4166 (5)	0.50024 (8)	0.0384 (7)
H13	1.152969	0.359944	0.494794	0.046*
C8	0.8942 (5)	0.5024 (4)	0.47567 (8)	0.0327 (6)
C7	0.8675 (6)	0.4483 (4)	0.41677 (8)	0.0355 (7)
C1	0.9865 (6)	0.4774 (4)	0.38438 (8)	0.0327 (6)
C6	0.8794 (6)	0.4209 (5)	0.35476 (9)	0.0370 (8)
H6	0.738063	0.367892	0.355958	0.044*
C5	0.9820 (6)	0.4433 (5)	0.32362 (8)	0.0424 (8)
H5	0.910596	0.406027	0.303881	0.051*
C4	1.1928 (6)	0.5221 (5)	0.32236 (8)	0.0394 (7)
C10	0.6189 (6)	0.5857 (5)	0.51662 (8)	0.0384 (7)
H10	0.483925	0.642600	0.521791	0.046*
C9	0.6957 (6)	0.5876 (5)	0.48333 (9)	0.0400 (8)
H9	0.613348	0.645774	0.466508	0.048*
C16	0.3731 (5)	0.5741 (5)	0.61941 (9)	0.0370 (7)
H16	0.233589	0.623998	0.624316	0.044*
C15	0.4492 (5)	0.5716 (5)	0.58628 (8)	0.0368 (7)

H15	0.358554	0.618626	0.569238	0.044*
C2	1.1985 (5)	0.5553 (4)	0.38240 (8)	0.0365 (7)
H2	1.272007	0.591248	0.402036	0.044*
C3	1.3003 (6)	0.5793 (5)	0.35129 (9)	0.0389 (7)
H3	1.440710	0.633865	0.349921	0.047*
O3	0.5380 (5)	0.4447 (5)	0.70399 (7)	0.0732 (10)

*Atomic displacement parameters (Å<sup>2</sup>)*

	$U^{11}$	$U^{22}$	$U^{33}$	$U^{12}$	$U^{13}$	$U^{23}$
Br1	0.0637 (2)	0.0753 (2)	0.03460 (15)	−0.00193 (19)	0.0122 (2)	0.0024 (2)
O2	0.0385 (12)	0.0495 (13)	0.0275 (10)	−0.0062 (10)	0.0031 (9)	−0.0048 (9)
O1	0.0510 (15)	0.0747 (18)	0.0459 (15)	−0.0271 (14)	0.0108 (12)	−0.0129 (14)
C21	0.069 (3)	0.101 (4)	0.041 (3)	0.004 (3)	0.015 (2)	0.003 (2)
O4	0.0532 (16)	0.092 (2)	0.0369 (15)	0.0124 (15)	0.0089 (12)	0.0039 (14)
C20	0.050 (2)	0.052 (2)	0.0323 (16)	−0.0042 (16)	0.0003 (15)	−0.0007 (14)
C17	0.0399 (16)	0.0391 (17)	0.0302 (14)	−0.0033 (13)	−0.0020 (13)	−0.0003 (13)
C18	0.0397 (17)	0.050 (2)	0.0351 (16)	0.0046 (15)	−0.0046 (13)	0.0008 (15)
C19	0.0328 (16)	0.050 (2)	0.0348 (16)	0.0074 (14)	−0.0039 (12)	0.0010 (14)
C14	0.0328 (13)	0.0256 (13)	0.0329 (15)	−0.0002 (12)	−0.0010 (12)	−0.0009 (11)
C11	0.0330 (14)	0.0247 (12)	0.0311 (14)	−0.0015 (11)	−0.0005 (12)	−0.0010 (11)
C12	0.0387 (16)	0.0393 (18)	0.0344 (16)	0.0076 (14)	−0.0010 (13)	0.0016 (13)
C13	0.0341 (16)	0.0447 (18)	0.0365 (17)	0.0087 (14)	0.0033 (13)	−0.0019 (13)
C8	0.0333 (15)	0.0322 (15)	0.0327 (15)	−0.0050 (12)	0.0044 (12)	−0.0031 (12)
C7	0.0390 (17)	0.0326 (15)	0.0350 (16)	−0.0014 (13)	0.0023 (13)	−0.0030 (13)
C1	0.0381 (15)	0.0279 (14)	0.0322 (15)	0.0001 (12)	−0.0005 (12)	−0.0015 (12)
C6	0.0348 (16)	0.0366 (16)	0.039 (2)	−0.0028 (12)	−0.0020 (14)	−0.0031 (14)
C5	0.0446 (18)	0.0495 (19)	0.0329 (17)	−0.0003 (15)	−0.0052 (14)	−0.0044 (14)
C4	0.0452 (19)	0.0421 (17)	0.0308 (16)	0.0024 (14)	0.0037 (13)	0.0025 (13)
C10	0.0381 (16)	0.0432 (18)	0.0339 (16)	0.0130 (14)	0.0028 (13)	0.0005 (13)
C9	0.0434 (19)	0.0443 (19)	0.0323 (15)	0.0120 (15)	−0.0019 (13)	0.0055 (13)
C16	0.0296 (16)	0.0448 (19)	0.0367 (16)	0.0039 (13)	0.0019 (12)	0.0009 (14)
C15	0.0353 (15)	0.0430 (18)	0.0322 (15)	0.0051 (14)	−0.0030 (12)	0.0058 (13)
C2	0.0357 (16)	0.0411 (17)	0.0327 (15)	−0.0014 (13)	−0.0026 (12)	−0.0019 (13)
C3	0.0340 (16)	0.0447 (18)	0.0379 (17)	−0.0030 (13)	0.0047 (13)	0.0006 (14)
O3	0.0623 (19)	0.125 (3)	0.0323 (14)	0.0227 (19)	−0.0003 (13)	0.0077 (16)

*Geometric parameters (Å, °)*

Br1—C4	1.884 (3)	C12—C13	1.384 (4)
O2—O2	0.000 (4)	C12—H12	0.9300
O2—C7	1.358 (4)	C13—C8	1.373 (5)
O2—C8	1.396 (4)	C13—H13	0.9300
O1—C7	1.195 (4)	C8—C9	1.373 (5)
C21—O4	1.452 (5)	C7—C1	1.480 (4)
C21—H21A	0.9600	C1—C2	1.390 (4)
C21—H21B	0.9600	C1—C6	1.397 (5)
C21—H21C	0.9600	C6—C5	1.385 (5)

O4—C20	1.331 (5)	C6—H6	0.9300
C20—O3	1.196 (5)	C5—C4	1.386 (5)
C20—C17	1.483 (5)	C5—H5	0.9300
C17—C16	1.379 (5)	C4—C3	1.376 (5)
C17—C18	1.387 (5)	C10—C9	1.394 (5)
C18—C19	1.376 (5)	C10—H10	0.9300
C18—H18	0.9300	C9—H9	0.9300
C19—C14	1.394 (4)	C16—C15	1.387 (4)
C19—H19	0.9300	C16—H16	0.9300
C14—C15	1.395 (4)	C15—H15	0.9300
C14—C11	1.484 (4)	C2—C3	1.384 (5)
C11—C12	1.392 (5)	C2—H2	0.9300
C11—C10	1.403 (4)	C3—H3	0.9300
C7—O2—C8	118.6 (3)	C9—C8—O2	121.2 (3)
O4—C21—H21A	109.5	C13—C8—O2	117.4 (3)
O4—C21—H21B	109.5	O1—C7—O2	123.0 (3)
H21A—C21—H21B	109.5	O1—C7—C1	125.5 (3)
O4—C21—H21C	109.5	O2—C7—C1	111.5 (3)
H21A—C21—H21C	109.5	C2—C1—C6	119.4 (3)
H21B—C21—H21C	109.5	C2—C1—C7	123.0 (3)
C20—O4—C21	117.2 (3)	C6—C1—C7	117.6 (3)
O3—C20—O4	123.1 (4)	C5—C6—C1	120.5 (3)
O3—C20—C17	124.5 (4)	C5—C6—H6	119.7
O4—C20—C17	112.4 (3)	C1—C6—H6	119.7
C16—C17—C18	118.7 (3)	C6—C5—C4	118.9 (3)
C16—C17—C20	122.7 (3)	C6—C5—H5	120.6
C18—C17—C20	118.5 (3)	C4—C5—H5	120.6
C19—C18—C17	120.5 (3)	C3—C4—C5	121.4 (3)
C19—C18—H18	119.7	C3—C4—Br1	119.6 (3)
C17—C18—H18	119.7	C5—C4—Br1	119.1 (3)
C18—C19—C14	121.9 (3)	C9—C10—C11	121.5 (3)
C18—C19—H19	119.0	C9—C10—H10	119.3
C14—C19—H19	119.1	C11—C10—H10	119.3
C19—C14—C15	116.8 (3)	C8—C9—C10	119.2 (3)
C19—C14—C11	121.8 (3)	C8—C9—H9	120.4
C15—C14—C11	121.4 (3)	C10—C9—H9	120.4
C12—C11—C10	116.7 (3)	C17—C16—C15	120.5 (3)
C12—C11—C14	122.2 (3)	C17—C16—H16	119.7
C10—C11—C14	121.1 (3)	C15—C16—H16	119.7
C13—C12—C11	122.3 (3)	C16—C15—C14	121.6 (3)
C13—C12—H12	118.9	C16—C15—H15	119.2
C11—C12—H12	118.9	C14—C15—H15	119.2
C8—C13—C12	119.2 (3)	C3—C2—C1	120.2 (3)
C8—C13—H13	120.4	C3—C2—H2	119.9
C12—C13—H13	120.4	C1—C2—H2	119.9
C9—C8—C13	121.1 (3)	C4—C3—C2	119.7 (3)
C9—C8—O2	121.2 (3)	C4—C3—H3	120.2

C13—C8—O2	117.4 (3)	C2—C3—H3	120.2
C21—O4—C20—O3	-4.2 (6)	O2—C7—C1—C2	2.7 (4)
C21—O4—C20—C17	176.9 (4)	O1—C7—C1—C6	0.2 (5)
O3—C20—C17—C16	-175.4 (4)	O2—C7—C1—C6	-178.2 (3)
O4—C20—C17—C16	3.5 (5)	O2—C7—C1—C6	-178.2 (3)
O3—C20—C17—C18	6.2 (6)	C2—C1—C6—C5	-0.5 (5)
O4—C20—C17—C18	-174.8 (3)	C7—C1—C6—C5	-179.7 (3)
C16—C17—C18—C19	-0.7 (5)	C1—C6—C5—C4	0.2 (5)
C20—C17—C18—C19	177.7 (3)	C6—C5—C4—C3	-0.5 (5)
C17—C18—C19—C14	0.2 (5)	C6—C5—C4—Br1	178.9 (3)
C18—C19—C14—C11	179.5 (3)	C12—C11—C10—C9	-0.6 (5)
C19—C14—C11—C12	6.1 (5)	C14—C11—C10—C9	179.5 (3)
C15—C14—C11—C12	-174.4 (3)	C13—C8—C9—C10	-0.3 (5)
C19—C14—C11—C10	-174.0 (3)	O2—C8—C9—C10	-174.5 (3)
C15—C14—C11—C10	5.5 (5)	O2—C8—C9—C10	-174.5 (3)
C10—C11—C12—C13	0.6 (5)	C11—C10—C9—C8	0.5 (5)
C14—C11—C12—C13	-179.5 (3)	C18—C17—C16—C15	1.0 (5)
C11—C12—C13—C8	-0.5 (5)	C20—C17—C16—C15	-177.3 (3)
C12—C13—C8—C9	0.3 (5)	C17—C16—C15—C14	-0.8 (5)
C12—C13—C8—O2	174.7 (3)	C19—C14—C15—C16	0.3 (5)
C12—C13—C8—O2	174.7 (3)	C11—C14—C15—C16	-179.2 (3)
C7—O2—C8—C9	-60.4 (4)	C6—C1—C2—C3	1.1 (5)
C7—O2—C8—C13	125.3 (3)	C7—C1—C2—C3	-179.8 (3)
C8—O2—C7—O1	-0.5 (5)	C5—C4—C3—C2	1.1 (5)
C8—O2—C7—C1	178.0 (3)	Br1—C4—C3—C2	-178.3 (3)
O1—C7—C1—C2	-178.9 (3)	C1—C2—C3—C4	-1.4 (5)
O2—C7—C1—C2	2.7 (4)		

### Hydrogen-bond geometry ( $\text{\AA}$ , $^\circ$ )

Cg1, Cg2 and Cg3 are the centroids of the aromatic rings C1–C6, C8–C13 and C14–C19, respectively

$D-H\cdots A$	$D-H$	$H\cdots A$	$D\cdots A$	$D-H\cdots A$
C3—H3 $\cdots$ Cg1 <sup>i</sup>	0.93	2.82	3.526 (4)	133
C6—H6 $\cdots$ Cg1 <sup>ii</sup>	0.93	2.83	3.523 (4)	133
C10—H10 $\cdots$ Cg2 <sup>iii</sup>	0.93	2.83	3.523 (4)	132
C13—H13 $\cdots$ Cg2 <sup>iv</sup>	0.93	2.87	3.552 (4)	131
C16—H16 $\cdots$ Cg3 <sup>iii</sup>	0.93	2.92	3.566 (4)	128
C19—H19 $\cdots$ Cg3 <sup>iv</sup>	0.93	2.99	3.623 (4)	127

Symmetry codes: (i)  $x-1/2, -y-1/2, z$ ; (ii)  $x+1/2, -y+3/2, z$ ; (iii)  $x+1/2, -y+1/2, z$ ; (iv)  $x-1/2, -y+3/2, z$ .